Available online at www.sciencedirect.com
ScienceDirect
Nuclear Instruments and Methods in Physics Research A 576 (2007) 204–208
NUCLEAR INSTRUMENTS & METHODS IN PHYSICS RESEARCH Section A
www.elsevier.com/locate/nima

Preliminary characterization of a single photon counting detection system for CT application

N. Belcari, M.G. Bisogni, C. Carpentieri, A. Del Guerra, P. Delogu, D. Panetta*, M. Quattrocchi, V. Rosso, A. Stefanini

Department of Physics, University of Pisa and INFN, Sezione di Pisa, Pisa, Italy

Available online 6 February 2007

Abstract

The aim of this work is to evaluate the capability of a single photon counting acquisition system based on the Medipix2 read-out chip for Computed Tomography (CT) applications in Small Animal Imaging. We used a micro-focus X-ray source with a W anode. The detection system is based on the Medipix2 read-out chip, bump-bonded to a 1 mm thick silicon pixel detector. The read-out chip geometry is a matrix of 256×256 cells, $55\,\mu m \times 55\,\mu m$ each. This system in planar radiography shows a good detection efficiency (about 70%) at the anode voltage of 30 kV and a good spatial resolution (MTF = 10% @ 16.8 lp/mm). Starting from these planar performances we have characterized the system for the tomography applications with phantoms. We will present the results obtained as a function of magnification with two different background medium compositions. The effect of the reconstruction algorithm on image quality will be also discussed.

Keywords: Single photon counting; Medipix2; MicroCT; Spatial resolution

1. Introduction

Computed Tomography (CT) is a very important tool for non-invasive 3D imaging of opaque objects. Dedicated CT scanners for inspection of small specimens with micrometric resolution (MicroCT) have been developed, finding applications in biomedical research [1] and in non-destructive testing (NDT) of materials and components [2].

In our laboratory, we have assembled a MicroCT scanner prototype for small animal imaging [3], based on a CCD + CsI:Tl detector. Recently, we have modified this prototype by substituting the CCD + CsI:Tl detector with a single photon counting detection system; the main goal of this study is to characterize the new prototype in terms of spatial resolution for various geometric configurations and to make a preliminary comparison of the performances of the two detection systems in CT.

*Corresponding author. Tel.: +39 050 2214 334; fax: +39 050 2214 333.
E-mail address: daniele.panetta@pi.infn.it (D. Panetta).

0168-9002/$ - see front matter
doi:10.1016/j.nima.2007.01.153

2. Materials and methods

The main components of the MicroCT prototype are: a micro-focus X-ray from Hamamatsu with tungsten anode, a peak voltage up to 60 kV and a maximum power of 10 W; a rotator/translator stage for the motion of the specimen; a 1 mm thick silicon pixel detector produced in collaboration with ITC-irst [4], operating at 240 V and bump-bonded to the Medipix2 chip. The detector is a matrix of 256×256 square cells, with $55\,\mu m$ side. Each of the electronic cells has a low noise preamplifier, two pulse height discriminators and a 13 bit pseudo-random counter [5]. The readout system is able to set both low- and high-energy thresholds, allowing the selection of an energy window in the X-ray output spectrum.

The aim of this work is to assess the spatial resolution capabilities, in different geometrical conditions, of a MicroCT scanner prototype based on the photon counting detection system described above. To do this, we used a simple phantom composed by a hollow plastic cylinder of 3 cm diameter and 1 mm wall thickness, in which we placed a tungsten wire of $20\,\mu m$ of diameter. The thin wire allows to directly measure the point spread function (PSF) of the system. In the first set of measurements the cylinder was filled with water, while in the second set it was left empty (i.e., the background medium around the wire was air). The use of different background media can affect the spatial resolution of the system because of different amounts of Compton scattering.

2.1. Tomographic acquisition

The measurements were carried out at various different magnification factors; this was possible by changing the longitudinal position of the phantom between source and detector. The total source–detector distance was left unchanged to 40 cm. The main drawback of the used detector is the relatively small active area ($1.4 \times 1.4\,\mathrm{cm}^2$). In order to obtain a sufficient field of view (FoV) in tomography, it was necessary to acquire projections of the object at many different detector positions for each angle of view (see Fig. 1). The number of detector positions per view varies from 3 up to 7, depending on the magnification factor. In all the tomographic acquisitions we used the following settings: $30\,\mathrm{kV_p}$, 0.25 mA, 2 s exposition time for each detector position, 1 mm Al filter, 480 angles.

2.2. Reconstruction software

Because of the small size of the detector in the axial direction, the scanning geometry of our prototype is a stacked-fan-beam geometry. After equalizing each planar image with the corresponding high statistical flat field, the fan-beam sinogram of each slice was formed, then a filtered backprojection (FBP) algorithm with ramp filter was applied [6]. Finally, the 3D image was composed by stacking all the reconstructed slices. Because we are interested in the imaging of very small objects, we have used properly reconstruction grid sizes in order to avoid aliasing in the tomographic images. Typically, we have used pixel size 5–6 times smaller than the natural pixel size set by the detector pitch and the magnification factor. Particular care was devoted to reconstruct the images using the right value of the center of rotation (CoR) displacement. This issue is very important for our pourposes because the measured PSF size is strongly dependent on the CoR shift.

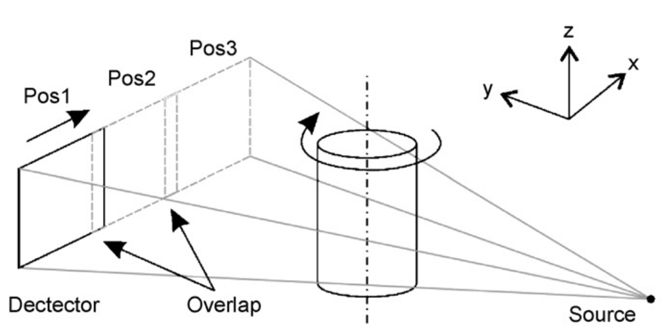

Fig. 1. Scanning geometry of the MicroCT prototype. Due to the small active area of the detector, a linear scanning of the object was necessary for each angle of view. A small overlap region (10 pixels) between adjacent detector positions was used. In the figure, only 3 positions are shown; depending on the object size and magnification factor, up to 7 positions could be used.

3. Theory

3.1. MTF model for the tomographic system

In the present discussion we assume that the system is shift-invariant, so we neglect the variations of the system response in the transaxial plane. If the imaging system is isotropic, i.e., if the spatial resolution does not depend on a particular direction selected in the image plane, the modulation transfer function (MTF) of the tomographic system can be expressed as

$$\mathrm{MTF}(f) = \Im_{1\mathrm{D}}\{\mathrm{LSF}(x)\}, \quad (1)$$

where $\Im_{n\mathrm{D}}$ denotes n-dimensional Fourier transform, and $\mathrm{LSF}(x)$ is the line spread function of the system. In CT it is easier to measure the PSF of the system instead of the LSF; in order to avoid calculation involving 2D Fourier transforms of the data, it is desirable to find a direct relation between MTF and a 1D central profile of the PSF. If $\mathrm{PSF}(x,y)$ is a circularly symmetric 2D Gaussian function with standard deviation σ, the LSF is a 1D Gaussian function with the same standard deviation σ. So we can write the following expression for the MTF of an isotropic shift-invariant tomographic system:

$$\mathrm{MTF}(f) = \Im_{1\mathrm{D}}\{\mathrm{PSF}(x,y)|_{y=0}\} = \prod_i \mathrm{MTF}_i(f) \quad (2)$$

where

$$\mathrm{MTF}_i(f) = \Im_{1\mathrm{D}}\{\mathrm{PSF}_i(x)|_{y=0}\} \quad (3)$$

is the MTF of the ith blurring component of the whole imaging system. For the sake of simplicity, in the above equations we have selected the PSF profile along the x-axis; because of the isotropy of the system, any other central profile could be selected.

The above equations allow us to measure the MTF of the system by simply taking the 1D Fourier transform of a central profile of the PSF. We can model the in-plane PSF as a circularly symmetric 2D Gaussian function, G2D, with standard deviation σ_{PSF}:

$$\mathrm{PSF}(x,y) = G_{2\mathrm{D}}(x,y;\sigma_{\mathrm{PSF}}). \quad (4a)$$

Assuming that all blurring components are Gaussian and isotropic in the transaxial plane, we can write

$$\sigma_{\mathrm{PSF}} = \sqrt{\sum_i \sigma_i^2} \quad (4b)$$

where σ_i is the standard deviation of the ith blurring component.